Biological evaluation of nano hydroxyapatite zirconia (HA-ZrO_2) composites for load bearing applications.

I.M. Brook*, C.O. Freeman, and S. Grubb

School of Clinical Dentistry, University of Sheffield, Claremont Crescent, Sheffield, S10 2TA, UK

N.M. Cummins, D.J. Curran, C.J. Reidy, and S Hampshire

University of Limerick, Materials and Surface Science Institute, National Technological Park, Limerick, Ireland

M.R. Towler

Alfred University, Inamori School of Engineering, Alfred University, 1 Saxon Drive, Alfred, NY14802

* Author to whom correspondence should be addressed. E-mail i.brook@sheffield.ac.uk

Abstract

The biological response of strontium (Sr) doped hydroxyapatite (HA) and hydroxyapatite-zirconia (HA-ZrO_2) composites produced by employing sol-gel technology, minimal ZrO_2 loadings and novel microwave sintering regimes thereby retarding decomposition, is reported. *In vitro* evaluations indicate that all materials induce a favourable response from rat osteosarcoma cells (ROS). *In vivo* evaluations show osteoconductivity and biocompatibility for both the Sr-HA and HA-ZrO_2. The materials did not cause any inflammatory response in bone. The Sr-HA displays better biocompatibility which may be a due to the incorporation of Sr and the formation of a surface apatite layer.

1. Introduction

We report the biological response of novel nano Sr-HA and HA-ZrO_2 composites designed for load bearing applications in the skeleton produced by employing sol-gel technology, minimal ZrO_2 loadings and novel microwave sintering regimes, thereby retarding decomposition (1,2). Three composites were evaluated *in vitro* using rat osteosarcoma (ROS) cells; a reproducible method of determining the response of cells in culture to test biomaterials (3). The two most promising materials were then further evaluated to assess the bone response to the test materials in a rat femur healing model (4).

HA is employed for repairing skeletal defects as it resembles the mineral phase of bone and is bioactive. However, its poor strength limits load-bearing applications. Mechanical properties can be improved by incorporating zirconia, but sintering at high temperature is required, resulting in HA decomposition and reduced bioactivity (5,6). At a critical point of dehydroxylation the process becomes irreversible and the HA begins to decompose to other calcium phosphates (7). Decomposition produces products such as tetracalcium phosphate [TTCP]{$Ca_4(PO_4)_2O$} which can further degrade to tri-calcium phosphate [TCP]{$Ca_3(PO_4)_2$} (8) and calcium oxide. In addition, studies of the stability of HA show that the presence of ZrO_2 serves to destabilise the HA structure at lower temperatures than would be seen without the oxide phase (9,10,11,12).

Sr^{2+} has a biological role in the body where it decreases the activity of bone resorbing osteoclasts and increases the activity of bone forming osteoblasts (13,14). In the HA lattice, Sr^{2+} replaces the cation Ca^{2+}, but due to the mismatch in atomic radii there is a lattice expansion (15,16) affecting the properties of the material. The presence of Sr^{2+} within HA is known to decrease the mechanical resistance of the ceramic in a linear manner (17); and may also increase the solubility of Sr-HA compared to HA. This increase in the solubility of the Sr-HA has been reported to have a positive effect on osteoblasts and reduce the number of osteoclasts due to the release of Sr^{2+} (18). In addition to Sr^{2+} release, increased Ca^{2+} release from Sr-HA is suggested to activate calcium channels and thus stimulate cell response (19). Also, increased solubility of the Sr-HA increases the possibility of increased interconnected porosity on its surface enhancing osseintegration (20,21) and interfacial bonding (22). Thus, although Sr-HA is a more resorbable material than HA, its possible increase in bioactivity and bonding to bone make it a more desirable material that could influence the quality of newly formed bone.

Zirconia exists in three different phases depending on temperature; monoclinic (M) at room temperature to 1170°C, tetragonal (T) between 1170°C and 2370°C and cubic (C) above this temperature (23). Upon cooling, the T-M transformation results in a volume expansion of approximately 4% and the associated stresses can result in cracking of pure zirconia. The addition of "stabilising oxides" such as CaO, MgO, Y_2O_3 and CeO_2 are required to stabilise the high temperature C/T phases at room temperature. The addition of small amounts of Y_2O_3 (2-3 mol%) to zirconia can result in the retention of a fully tetragonal phase at room temperature known as tetragonal zirconia polycrystals (TZP) (24). Yttria stabilized TZP (Y-TZP) has various inherent characteristics such as low porosity, high density, high bending and compression strengths, low coefficient of thermal expansion and chemical stability which make it suitable for clinical applications (25).

The aim of this study was to evaluate the *in vivo* and *in vitro* response of these novel Sr-HA and HA-ZrO_2 composites designed for skeletal load bearing applications.

2. Materials and Methods

2.1. Materials

A simple precipitation method previously described by Jarcho *et al*. (26) was used for the HA, which was then modified to produce Sr-HA.

Pure-HA

Calcium nitrate hydrate ($Ca(NO_3)_2.4H_2O$) (78.72g) was dissolved in 600ml of distilled water which was made basic by the addition of 10ml of ammonium hydroxide (NH_4OH). The mixture was stirred vigorously and raised to the desired temperature of 25^oC under the same stirring conditions.

10wt% Sr-HA:

$Ca(NO_3)_2.4H_2O$ (71.11g) was dissolved in 600ml of distilled water which was made basic by the addition of 10ml of NH_4OH under vigorous stirring conditions. Once the $Ca(NO_3)_2.4H_2O$ had dissolved, 7.08g of strontium nitrate hydrate ($Sr(NO_3)_2.4H_2O$) was added to the $Ca(NO_3)_2.4H_2O$ and the mixture was raised to the desired temperature of 25^oC under the same stirring conditions.

Di-ammonium hydrogen orthophosphate ($(NH_4)_2HPO_4$) (26.41g) was made basic in 1066ml of water by the addition of 25ml of NH_4OH, and brought to the desired temperature of 25^oC. The $Ca(NO_3)_2.4H_2O$ and $(NH_4)_2HPO_4$ based solutions were stirred vigorously before synthesis to ensure the reagents were completely dissolved. To determine this, visual inspection of the solution was conducted for un-dissolved reagent particulates. Under continued vigorous stirring, the $(NH_4)_2HPO_4$ solution was added drop-wise from a glass funnel into the $Ca(NO_3)_2.4H_2O$ solution over a 60 minutes interval. Throughout the synthesis the pH was kept above 10.0 by the addition of NH_4OH at constant intervals to avoid a large pH change to the system. Once the drop-wise addition was completed, the solution was kept at the synthesis temperature for one hour under the same temperature and vigorous stirring conditions, effectively giving an ageing time of one hour. The sample was then left to stand for 24 hours at room temperature. The supernatant was removed and replaced with fresh distilled water, re-stirred for one hour and left to stand again for 24 hours. This procedure was performed three times to remove any unwanted residue from the precipitate. The supernatant was removed a final time and replaced with distilled water and spun for 15

minutes. The suspension was then filtered under vacuum, using a Buchner filter and distilled water until the ammonia was removed. The filter cake was then removed from the filter and placed into a beaker and dried in a fan assisted oven at 85^{o}C for 20 hours. The dry precipitate were then crushed by pestle & mortar and sieved through a 90µm stainless steel sieve.

The sieved HA was mixed with 3 mol% Y_2O_3 doped ZrO_2 (3Y-TZP) (Tosoh Corporation, Japan) using a dry ball-milling technique with alumina media for 6 h to create batches of composite powders with 5 and 10 wt % ZrO_2 additions as described elsewhere [2]. The test bodies of Sr-HA and ZrO_2-HA were prepared by pressing 1.3g of powder in a 20mm diameter stainless steel die. The green bodies were then densified using a hybrid microwave sintering furnace developed at the University of Limerick (Limerick, Ireland). The device has a peak power output of 1.125kW and utilises silicon carbide (SiC) as a susceptor medium to facilitate hybrid heating. Firings were performed at 1200^{o}C (±20^{o}C) with a hold time of 1 hour and subsequently left to furnace cool.

HA-A: contained HA doped with 10mol% Sr of the total calcium content. ***HA-B:*** contained HA with 5wt% ZrO_2 (3Y-TZP), and ***HA-C:*** HA with 10wt% ZrO_2 (3Y-TZP). Discs of HA-A, HA-B and HA-C were 8mm in diameter and 2mm in thickness. The irregular sized granules of HA-A and HA-B were in the range 90-350µm. The control discs were composed of heat cured acrylic.

2.2 X-Ray Diffraction (XRD)

The HA powder was pressed into ethyl-cellulose pellets using a 32mm ø stainless steel die. These were then placed in the X-ray Diffractometer (Philips X'Pert) for an initial scan covering a range of 10^{o} to 70^{o} 2θ, with a step size of 0.083^{o} and a step time of 120.015 seconds. The XRD patterns were then matched to patterns in the JCPDS using the X'Pert software.

2.3 X-Ray Fluorescence (XRF)

XRF is used to determine the chemical composition of a material (Ceram, Stoke-on-Trent, UK). A full report was received along with the calcium to phosphate ratio (Ca/P).

2.4 X-Ray Photoelectron Spectroscopy (XPS)

XPS measurements were done on a Kratos AXIS 165 spectrometer (Kratos Analytical, Shimadzu Corporation, Japan) with a monochromatic Al source of spot size 1 mm diameter. The X-Ray Gun was run at 150W (10 mA, 15kV) with mono Al K_α of 1486.58 eV. The Pass Energy was 160 eV for survey spectra and 20 eV for narrow regions with a vacuum compatibility of 10^{-8} Torr. The samples were scanned for 50ms (dwell) and 100ms (region) with an electron volt energy of 1 eV (dwell) and 0.05 eV (region). The spectra were collected in the normal to the surface direction with a detection limit of 0.1-0.5%. Construction and peak fitting of synthetic peaks in narrow region spectra used a Shirely type background and the synthetic peaks were of a mixed Gaussian-Lorenzian type. Relative sensitivity factors used were from the CasaXPS library containing Scofield cross-sections. RSF values used for individual peaks were given in excel sheets, which were used to tabulate and graph the data.

2.5. Cell culture

Immortalized rat osteosarcoma cells (ROS 17/2.8, Merck Inc.) were cultured in DMEM supplemented with 10% (v/v) fetal calf serum (BioSera Ltd., Ringmer, UK), 2mM L-glutamine, 100 units/ml penicillin, 100 μg/ml streptomycin and 250 μg/ml amphotericin B (Sigma, Poole, UK). Cells were incubated at 37°C in 5% CO_2 in tissue culture flasks and passaged by incubating with trypsin-EDTA (Sigma, Poole, UK).

2.6. Alamar Blue assay

Discs (acrylic, HA-A, HA-B and HA-C) were sterilised in 70% (v/v) ethanol, before being washed in PBS three times and placed into 24 well plates. ROS cells (1×10^4) were added onto the discs and incubated at 37°C in 5% CO_2. After 48 or 72 hours the media was replaced with media containing 10% alamar blue, covered with foil and incubated. After 4 hours the fluorescence (λ_{ex} = 540 nm, λ_{em} = 585 nm) was measured using an Infinite M200 plate reader with Magellan Software (Tecan, Switzerland).

2.7. DNA Quantification

Cells were lysed by repeated freeze thawing using molecular biology grade water and the amount of DNA was quantified using a fluorescent DNA Quantification Kit (Sigma). Briefly, unknown DNA samples were mixed with 2 μg/ml bisBenzimide H33258 solution and the fluorescence (λ_{ex} = 360 nm, λ_{em} = 460 nm) was measured using an Infinite M200

plate reader with Magellan Software (Tecan, Switzerland). These readings were then compared to standard curves to determine the amount of DNA in the samples.

2.8. Scanning electron microscopy (SEM)

Discs were fixed in 2.5% glutaraldehdye in 0.1 M phosphate buffer overnight at 4°C, washed three times in 0.1 M phosphate buffer and fixed in 2% aqueous osmium tetroxide for 2 hours at room temperature. Specimens were then dehydrated through a graded series of ethanol at room temperature and air dried overnight. Once dry, samples were mounted on stubs, attached with Sticky Tabs, and coated with approximately 25 nm of gold in an Edwards S150B sputter coater. Specimens were examined in a Phillips/FEI XL-20 SEM at an accelerating voltage of 20Kv.

2.9. Surgery

Juvenile male Wistar rats aged 4-6 weeks at the time of surgery were used for this study. Animals were housed in groups in conventional laboratory conditions and provided with standard laboratory food and water *ad-libitum.*

Animals were anaesthetised using Isoflurane in oxygen; under aseptic conditions the mid-shaft of the right femur was exposed using sharp and blunt dissection and a defect created using a 1mm diameter round stainless steel dental bur running at slow speed in a dental handpiece under saline irrigation. Approximately 4 - 8 granules (90-350µm) of a single test material were placed into the bone defect using fine tweezers, (n=6 per material).

Wounds were closed using resorbable sutures at 28 days. Animals were sacrificed using a schedule one method. The right femurs were dissected free and placed in formalin. The femurs were demineralised in formic acid and processed to paraffin embedded sections stained with haematoxylin and eosin. Evaluation of the bone response was carried out using conventional light microscopy.

2.10. Statistical Analysis

The differences between groups were analysed by the Mann-Whitney U test (GraphPad Prism version 5.01 for Windows, GraphPad Software, San Diego, CA, www.graphpad.com). The results were considered statistically significant at a P value of ≤ 0.05

3. Results

3.1 Powder characterisation

The stoichiometric quality of the laboratory produced HA was investigated using XRD and XRF analysis techniques. XRD analysis matched the laboratory synthesised HA to JCPDS card 09-0432 while the XRF results determined the Ca/P ratio to be 1.66. From these results it was determined that the HA synthesis procedure produces near stoichiometric quality HA. The ratio of Ca^{2+} to Sr^{2+} was determined using XPS as 19.43% to 1.99% respectively in the Sr-HA with 10% Sr^{2+} substituted for the total Ca^{2+} content. This ratio of 20:2 indicates that the there was near total substitution of the Sr^{2+} ions into the HA lattice in place of the Ca^{2+} ions.

3.2. Cell Viability (Incubation with Alamar Blue)

Initially at 48 hours, differences were seen in cell viability when comparing cells grown on the test materials and tissue culture plastic (100%). Cells grown on HA C (74%; p,0.01) were the least viable followed by HA B (85%; p,0.01) and then HA A (90%; $p<0.05$). However, after 72 hours of culture these differences were less marked and there was no significant difference in cell viability between all of the test materials (Figure 1).

a.

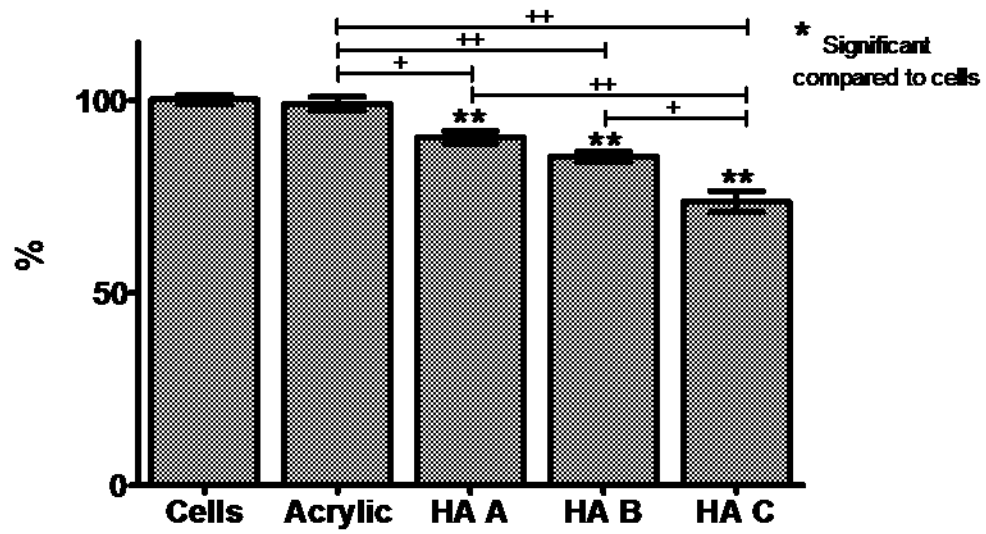

b.

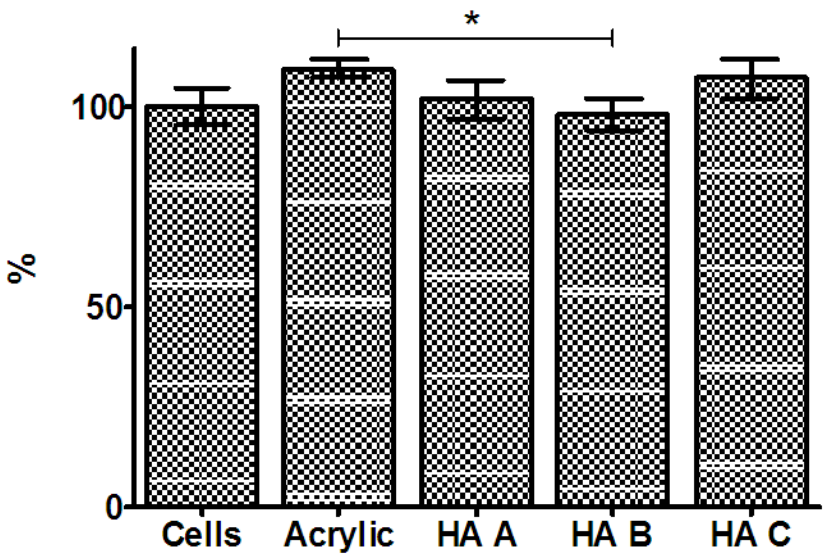

Figure 1. % Cell viability a) after 48 hours and b) 72 hours compared to cells grown on tissue culture plastic (100%). Mean ± SEM, n = 6 discs, + $p < 0.05$, ++ $p < 0.01$, ** $p < 0.01$ compared to tissue culture plastic control, Mann-Whitney)

3.3. DNA Quantification

DNA quantification showed that there was no significant difference between cells grown on acrylic and cells grown on the test materials after 48 and 72 hours (Figure 2). After 72 hours, there was a significant difference in the amount of DNA between cells grown on HA A and cells grown on HA B or HA C ($p<0.01$)

a.

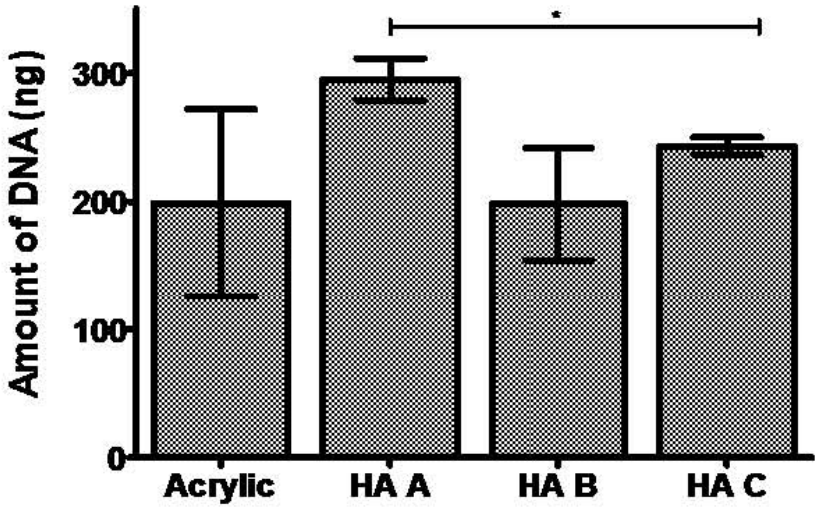

b.

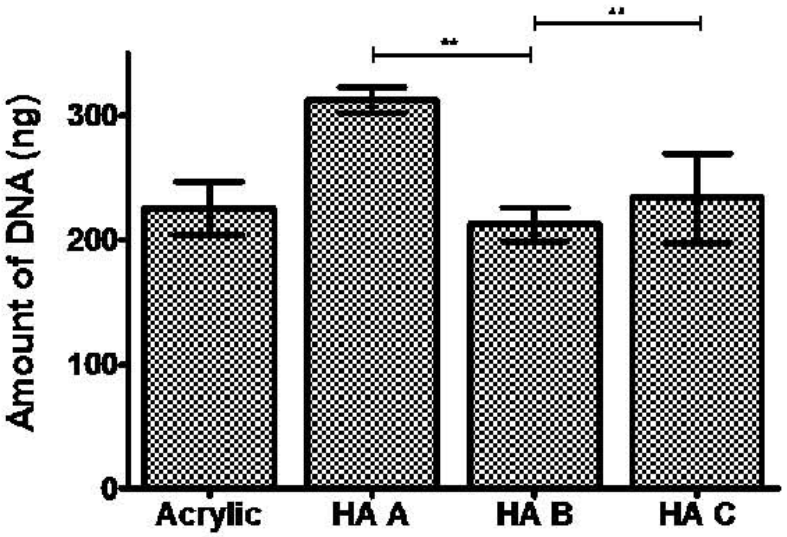

Figure 2 Amount of DNA a) after 48 hours and b) 72 hours. Mean ± SEM, n = 6 discs, * $p < 0.05$, ** $p < 0.01$, Mann-Whitney.

3.4. Qualitative Examination: SEM

The initial appearance of the materials surface prior to exposure to culture media, the effect of incubation with media and exposure to media and ROS cells are shown in figure 3.

Cells migrated onto and colonised all of the materials. Incubation with culture media alone for 72hours had no effect on the surface appearance of acrylic, HA-B and HA-C; however there was an alteration in the surface of HA-A with the deposition of a homogeneous crystalline layer (Figure 3). After culture with ROS cells for 72 hours cells had migrated onto and attached closely to the surface of all materials and were forming a confluent layer which was more complete on the acrylic and HA-A discs (Figure 3).

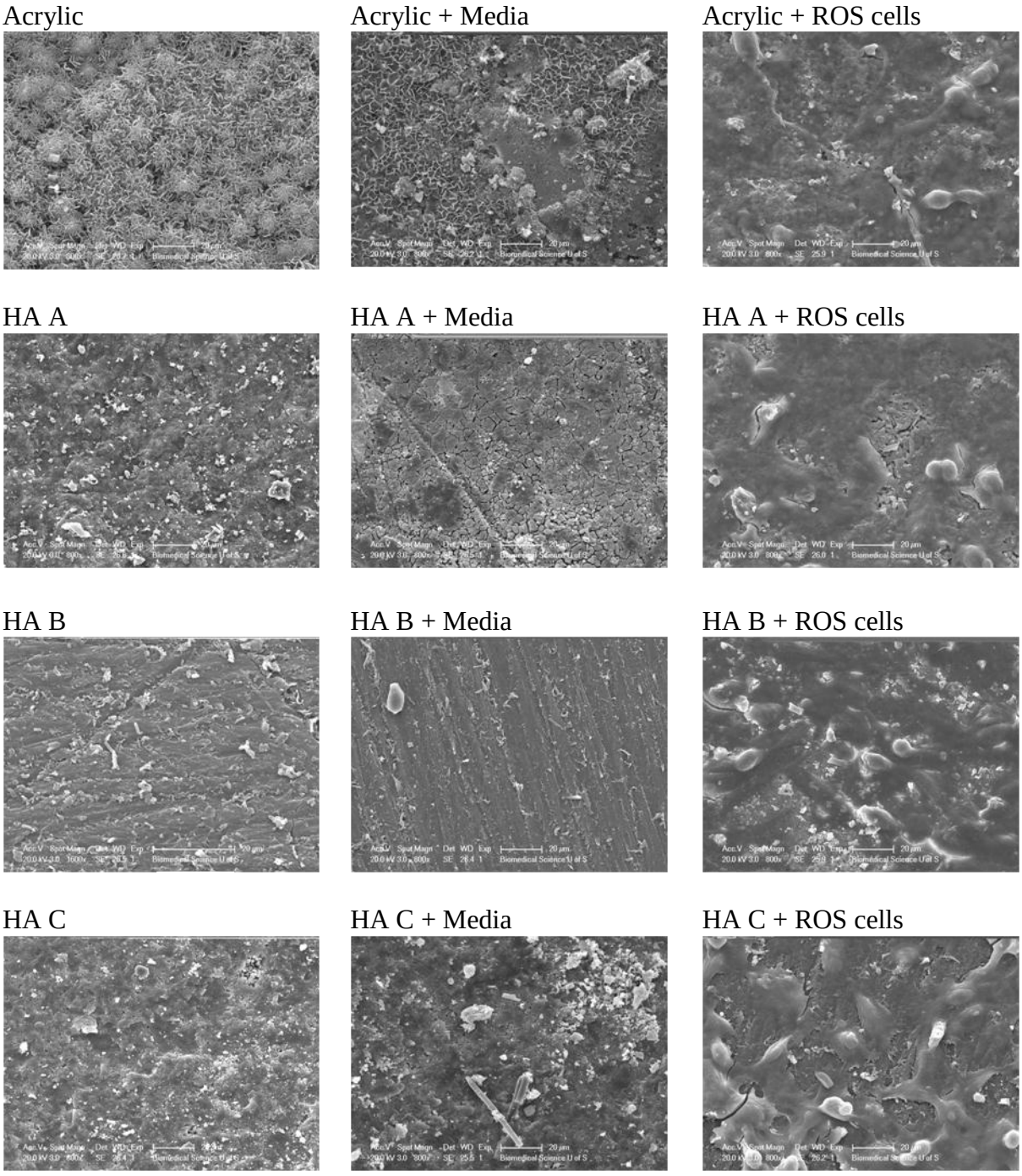

Figure 3. SEM images of discs (Acrylic, HA-A, HA-B and HA-C) initial appearance, after culturing for 72hours with tissue culture media or media and ROS cells (Scale bars 20 µm)

3.5. Surgery (light microscopy)

The histological features were similar for both HA-A and HA-B. At 4 weeks, all surgical sites were well healed and the cortical defect was closed and filled with lamellar bone. In some instances, particulate material was seen in this region and was in direct contact with bone. There was no evidence of an inflammatory response in any of the sections examined and the materials were well tolerated by bone and marrow tissue. The granules of material were in direct contact with either bone or normal marrow tissue (Figures 4 and 5). Where material was in direct contact with the endosteal bone, the bone was in continuity with the material (Figure 4c and 5b), in other areas there was a thin rim of bone around the particles (Figure 5b) and sometimes bone bridges between granules (Figure 4b). There was no evidence of resorption of either material. Where material was seen at the bone / connective tissue interface, a thin layer of fibrous connective tissue was seen over the material (Figure 4c)

A

B

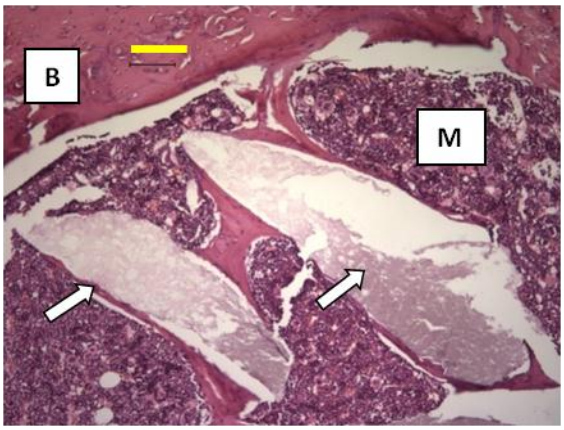

C

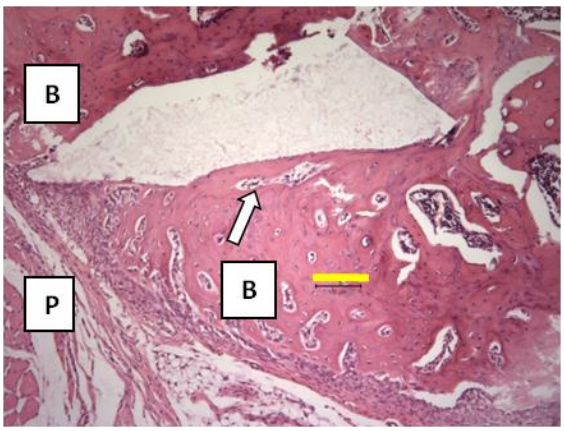

Figure 4 Haematoxylin and eosin stained section of HA-A implanted for 4 weeks into rat femora: (a) Low power, scale bar 1 mm, (b) and (c) medium power scale bar 100 µm. There is normal bone (B) and marrow (M) in close contact with HA-A (arrowed) with bone bridges between granules and between HA-A and the endosteal bone. Where material is seen to encroach on the overlying periosteal tissue it is covered by a layer of periosteum with no evidence of inflammation (P).

A

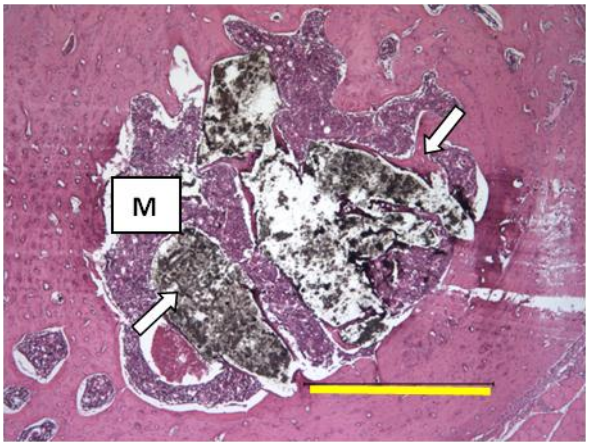

B

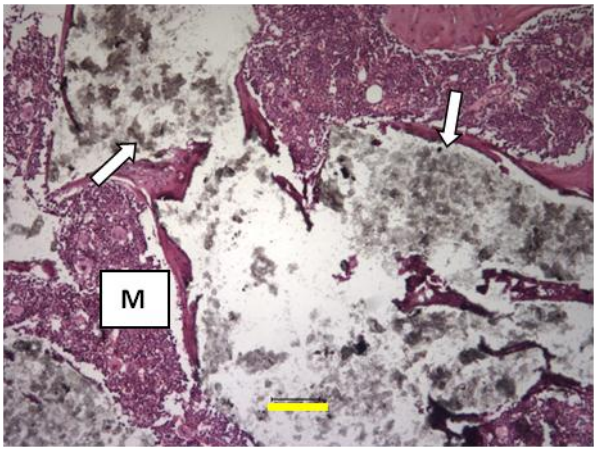

Figure 5 Haematoxylin and eosin stained section of HA-B implanted for 4 weeks into rat femora: (a) Low power, scale bar 1mm (b) medium power scale bar 100 µm. There is normal bone and marrow in close contact with HA-B (arrowed) with bone encapsulating the granules in the marrow space (M).

4. Discussion

The *in vitro* evaluation indicated that all three test materials induced a favourable response in the ROS cells with some evidence that the order of "biocompatibility" was:

$$\text{HA-A} > \text{HA-C} \geq \text{HA-B}.$$

HA-A may present better biocompatibility due to the variably observed deposition of material onto the surface which may have been an apatite layer observed by others on Sr-HA (27). Reduced zirconia content has also been reported to be associated with improved bone response in HA-ZrO_2 composites (28). HA-A also benefits from the incorporation of strontium (29).

The animal model used to assess the bone response to the test materials was the rat femur healing model, which is well established; this and the similar rat tibia model have been regularly used by our group and others (12,29). A defect in the immature rat femur will heal rapidly and implanted materials will often encourage increased bone formation in the medullary space; this region is normally occupied by marrow and has little trabecular bone except for the proximal and distal end of the bone. This model is useful for establishing whether a material will elicit a favourable or unfavourable response in bone. Those that excite an unfavourable response in this model are unlikely to be worthy of more long term studies. This model is useful as an early screen for new materials intended for medical implantation. ***HA-A:*** (Hydroxyapatite doped with 10mol% Strontium of the total Calcium content and ***HA-B:*** (HA with 5wt% ZrO_2 (3Y-TZP)) both elicited a favourable osteoconductive response in bone and would appear suitable for further evaluation in more rigorous non healing models. The materials appears not to have caused any inflammatory response in bone, but if excess material were to escape into soft tissue a different response may be elicited and care should be taken to interpret these results in the context of bone only.

5. Conclusion

- *In vitro* evaluation indicated that all three test materials induced a favourable response in the ROS cells, the order of 'biocompatibility' was HA-A>HA-C≥HA-B
- HA-A may have better biocompatibility due to incorporation of strontium and the formation of a surface layer on exposure to simulated body fluid – tissue culture media.
- *In vivo* evaluation showed both HA-A and HA-B materials to be osteoconductive and biocompatible in the model used.

Acknowledgement

Funded by the Enterprise Ireland Technology Development fund (contract, TD/2006/328).

References

1. Curran DJ, Fleming TJ, Kawachi G, Ohtsuki C, Towler MR. Characterisation and mechanical testing of hydrothermally treated HA/ZrO_2 composites. J. Mater. Sci. Mater. Med. 2009; doi: 10.1007/s10856-009-3801-6

2. Curran DJ, Fleming TJ, Towler MR, Hampshire S. Mechanical properties of hydroxyapatite–zirconia compacts sintered by two different sintering methods. J. Mater. Sci. Mater. Med. 2009; doi: 10.1007/s10856-009-3974-z

3. Bandyopadhyay-Ghosh S, Reaney IM, Brook IM, Hurrell-Gillingham K, Johnson A, Hatton PV. In vitro biocompatibility of fluorcanasite glass-ceramics for bone tissue repair. J Biomed Mater Res. 2007; 80(1):175-83.

4. Towler MR, Boyd D, Freeman C, Farthing P. Brook IM. Comparison of in vitro and in vivo bioactivity of SrO-CaO-ZnO-SiO2 glass grafts. J. Biomater. App. 2009;23:561-72.

5. Kim HW, Noh YJ, Koh YH, Kim HE. Enhanced performance of fluorine substituted hydroxyapatite composites for hard tissue engineering. J. Mater. Sci. Mater. Med. 2003;14:899-904.

6. Hing KA, Gibson IR, Di Silvio L, Best SM, Bonfield W. Effect of variation in Ca:P ratio on cellular response of primary human osteoblast-like cells to hydroxyapatite-based ceramics. Bioceramics. 1998;11:293-6.

7. Cihláø J, Buchal A, Trunec M. Kinetics of thermal decomposition of hydroxyapatite bioceramics. M. J. Mater. Sci. 1999;34:6121-31.

8. Bernache-Assollant D, Ababou A, Champion E, Heughebaert M. Sintering of calcium phosphate hydroxyapatite $Ca_{10}(PO_4)_6(OH)_2$ I. Calcination and particle growth. J. Euro. Ceram. Soc. 2003;23:229-41.

9. Silva VV, Lameiras FS, Dominguez RZ. Microstructural and mechanical study of zirconia-hydroxyapatite composite ceramics for biomedical applications. Composites Science and Technology, 2001;61(2):301-10.

10. Kim HW, Knowles JC, Li LH, Kim HE. Mechanical performance and osteoblast-like cell response of fluorine-submitted hydroxyapatite and zirconia dense composite. Journal of Biomedical Materials Research Part A. 2005; 72A(3):258-68.

11. Inuzuka M, Nakamura S, Kishi S, Yoshida K, Hashimoto K, Toda Y, Yamashita K. Hydroxyapatite-doped zirconia for preparation of biomedical composites ceramics. 2004;172(1-4):509-13.

12. Heimann RB, Vu TA. Effect of CaO on thermal decomposition during sintering of composite hydroxyapatite-zirconia mixtures for monolithic bioceramic implants. J. Mater. Sci. Lett. 1997;16:437-9.

13. M. Matsuyuki, H. Murata. Strontium substitution in bioactive calcium phosphates: A first-principles study. J. Phys. Chem. 2009;113:3584-89

14. Canalis E, Hott M, Deloffre P, Tsouderos Y, Marie PJ. The divalent strontium salt S12911 enhances bone cell replication and bone formation in vitro. Bone 1996;18:517-23.

15. J. Christofferson, M.R. Christofferson, N. Kolthoff, O. Barenholdt. Effects of strontium ions on growth and dissolution of hydroxyapatite and on bone mineral detection. Bone. 1997;20:47-54.

16. Bigi A, Boanini E, Capuccini C, Gazzano M. Strontium-substituted hydroxyapatite nanocrystals. Inorganica Chimica. Acta. 360. 2007;36:1009-16.

17. Ravaglioli A, Krajewski A. Bioceramics: materials, properties, applications. 1st ed. New York: Springer: 1992.

18. Capuccini C, Torricelli P, Sima F, Boanini E, Ristoscu C, Bracci B, Socol G, Fini M, Mihailescu IN, Bigi A. Strontium-substituted hydroxyapatite coatings synthesized by pulsed-

laser deposition: In vitro osteoblast and osteoclast response. Acta Biomaterialia. 2008;4:1885-93.

19. Columbe J, Faure H, Robin B, Raut M. In vitro effects of strontium ranelate on the extracellular calcium-sensing receptor. Biochemical and Biophysical Research Communications. 2004;323:1184-90

20. Chang BS, Lee CK, Hong KS, Youn HJ, Ryu HS, Chung SS, Park KW.Osteoconduction at porous hydroxyapatite with various pore configurations. Biomaterials 2000;21:1291-8.

21. Erbe EM, Marx JG, Clineff TD, Bellincampi LD. Potential of an ultraporous ß-tricalcium phosphate synthetic cancellous bone void filler and bone marrow aspirate composite graft. European Spine Journal 2001;10(S2):141-6.

22. Ni GX, Chiu KY, Lu WW, Wang Y, Zhang YG, Hao LB, Li ZY, Lam WM, Lu SB, Luk KDK. Strontium-containing hydroxyapatite bioactive bone cement in revision hip arthroplasty. Biomaterials 2006; 27(24): 348-55.

23. Piconi C, Maccauro G. Zirconia as a ceramic Biomaterial. Biomaterials 1999;20(1):1-25.

24. Gupta TK, Bechtold JH, Kuznickie RC, Cadoff LH, Rossing BR. Stabilization of tetragonal phase in polycrystalline zirconia. J Mater Sci 1977;12:2421-6.

25. Hisbergues M, Vendeville S, Vendeville P. Zirconia: Established facts and perspectives for a biomaterial in dental implantology. J. Biomed. Mater. Res., Part B 2008;88(2):519-29.

26. Jarcho M, Bolen CH, Thomas MB, Bobick J, Kay JF, Doremus RH. Hydroxylapatite synthesis and characterization in dense polycrystalline form. J. Mater. Sci. 1976;11:2027.

27. Wong KL, Wong CT, Liu WC, Pan HB, Fong MK, Lam WM, Cheung WL, Tang WM, Chiu KY, Luk KDK, Lu WW. Mechanical properties and *in vtiro* response of strontium containing hydroxyapatite/polyetheretherketone composites. Biomaterials. 2009;30(23-24):3810-3817.

28.Lee TM, Tsai RS, Chang E, Yang CY, Yang MR. Biological responses of neonatal rat calvarial osteoblasts on plasma-sprayed HA/ZrO_2 composite coating. J. Mater. Sci. Mater. Med. 2002;13(3):281-7.

29. Zreiqat H, Ramaswamy Y, Wu C , Paschalidis A, Lu Z, James B, Birke O, McDonald M, Little D, Dunstan CR. The incorporation of strontium and zinc into a calcium–silicon ceramic for bone tissue engineering. 2010;doi:10.1016/J.Biomaterials.2010.01.024